

Temperature Dependence of the Refractive Index Depth Profile and of the Mode Field of Integrated-optical Polymeric Waveguides Fabricated by UV Excimer Laser

M. A. Shams El-Din¹, H. H. Wahba¹, C. Wochnowski^{2*}, F. Vollertsen³

¹Physics Department, Faculty of Science, University of Damietta, New Damietta, Egypt

^{2*}former: BIAS (Bremer Institut für Angewandte Strahltechnik), Bremen, Germany

³BIAS (Bremer Institut für Angewandte Strahltechnik), Bremen, Germany

¹mamdoh.dom@gmail.com; ^{2*}cawochnowski@gmail.com; ³vollertsen@bias.de

Abstract

In this paper, a temperature controlled UV-laser lithographic method for the fabrication of integrated-optical polymeric waveguides is presented. The fabricated integrated-optical polymeric waveguides are examined at different processing temperatures. The influence of the temperature on the refractive index depth distribution and thus on the mode field distribution, the number of modes and the effective refractive index of each mode, respectively, is investigated. The refractive index depth profile of the integrated-optical polymeric waveguides is examined by using the Mach-Zehnder interferometric method and an image processing technique. The interference phase differences are extracted in order to determine the refractive index depth profiles of the fabricated optical waveguides. After determining the refractive index depth distribution experimentally, the data of the refractive index depth distribution are employed to calculate the mode field distribution, mode numbers and the effective refractive indices.

Keyword

Polymer Integrated Optics; UV-excimer Laser Lithography; Mach-Zehnder-interferometry; Refractive Index Depth Distribution

Introduction

The fabrication of integrated optical waveguides will be a very crucial technology for optical communications and sensing devices in the near future. However, it is absolutely necessary to have accurate knowledge about the optical waveguide parameters in technological applications.

In recent years, polymeric integrated optics has shifted to the focus of interest due to the low material cost and simple handling and processing of polymers during the manufacturing process. Mainly, PMMA is a very promising material to be used as a basic material to

produce optical waveguides and gratings [Baker, 1993; Eldada, 2000; Ma, 2002; Vollertsen, 2004].

The UV-laser lithographic fabrication method of integrated-optical waveguides has been well-recognized. In particular, UV excimer laser has been used to irradiate homogeneous slabs of PMMA in order to modify the refractive index locally in a controllable way at the polymeric substrate surface [Wochnowski, 2000; Shams-Eldin, 2004; Shams-Eldin, 2005; Koerdt, 2009; Wochnowski, 2008; Wochnowski, 2005]. Thus integrated-optical waveguides can be directly laser-written into the surface of polymeric substrates by employing lithographic masks. Thereby, it is very important that the refractive index is modified in a controllable way by using specific conditions during the irradiation process in order to obtain the desired waveguiding structures [Wochnowski, 2000]. The UV photons of the incident laser radiation interact with the molecules of the polymeric material due to UV-photon-induced processes [Wochnowski, 2000; Shams-Eldin, 2004; Shams-Eldin, 2005; Wochnowski, 2008; Wochnowski, 2005], so the refractive index at the surface of the PMMA slabs is changed in the irradiated area. The refractive index depth distributions of the UV-irradiated PMMA slabs/ waveguides have been examined by Mach-Zehnder interferometry technique. It has been shown that the refractive index depth profile in the irradiated area is featured by an unexpected extraordinary shape.

Today, it is well-known that the modified area consists of two zones according to former work [Shams-Eldin, 2004; Shams-Eldin, 2005]. The first zone has a graded refractive index variation (like parabolic shape). The second zone appears as a nearly Gaussian shape (more

details are given later, see figure (1 and 2)). Generally, the refractive index depth profile can be approximated by several kinds of functions; the complementary error function, the Gaussian function or a simple exponential function or it may be of a shape not describable by any simple mathematical function [Wahba, 2009; Crank, 1956; Kaminow, 1973, Giallorenzi, 1973].

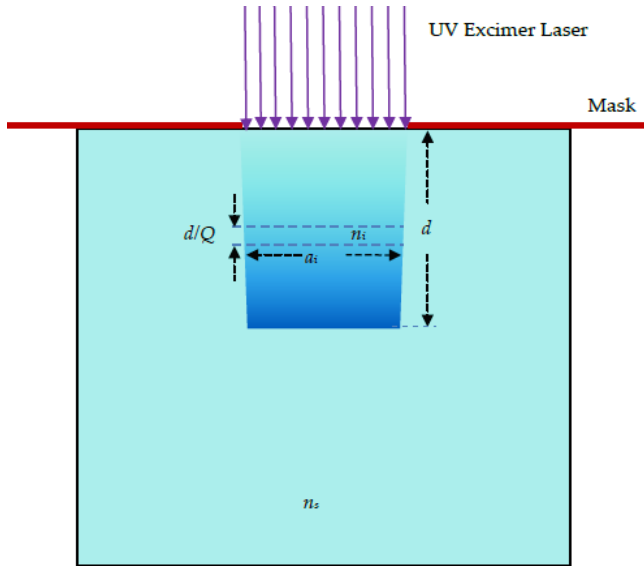


FIGURE 1 THE CROSS SECTIONAL AREA OF THE FABRICATED WAVEGUIDE BY UV EXCIMER LASER LITHOGRAPHIC METHOD IN A SLAB OF PMMA.

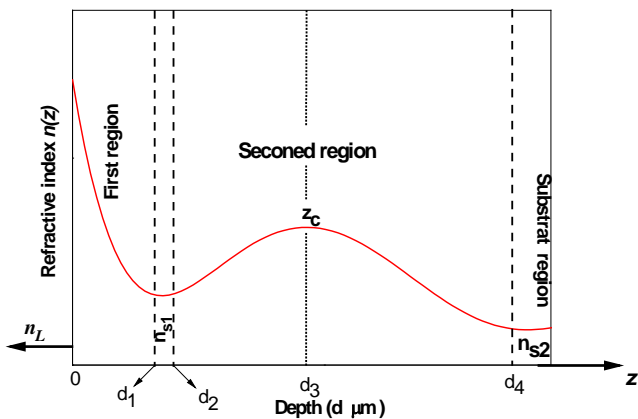


FIGURE 2 THE WAVEGUIDE CONFINED BETWEEN LIQUID AND SUBSTRATE MEDIA, ARRANGED SUCH THAT THE REFRACTIVE INDEX $N(Z)$ IS LARGER THAN THAT OF THE SURROUNDING MEDIA (n_L) AND (n_{s2}).

The reason for this extraordinary shape of the refractive index depth distribution is due to several divers UV-photon induced processes which occur simultaneously and/or subsequently during the UV-irradiation period in different depths at the surface and/or inside the bulk of the polymeric material. These UV-photon induced processes are discussed in details in [Wochnowski, 2000; Shams-Eldin, 2004; Shams-Eldin, 2005; Wochnowski, 2008; Wochnowski, 2005].

In former authors' works about the refractive index

depth distribution, the investigation is done by Mach-Zehnder interferometer [Shams-Eldin, 2004; Shams-Eldin, 2005; Wochnowski, 2008; Wochnowski, 2005]; and the produced interferograms were recorded manually. The contour lines of the interferograms were used to calculate the refractive index profile of the waveguides.

Recently, the refractive index distribution of GRIN optical fibers was investigated by Mach-Zehnder interferometry based on digital holography as well as on a computer-based image processing [Wahba, 2009]. By this means, optical phase differences were used to calculate the refractive index distributions of the samples by computer [Wahba, 2009]. It has been shown that in case of Mach-Zehnder interferometric method based on digital holography and on computer-based image processing, the accuracy of the obtained refractive indices data are far more precise than that determined by the manually-based Mach-Zehnder interferometry featured by the contour lines method [Shams-Eldin, 2004; Shams-Eldin, 2005; Wochnowski, 2008; Wochnowski, 2005].

However, it is crucial for the design and operation of integrated-optical components to know the precise mode field distribution, the exact number of modes and the effective refractive indices of each mode of the waveguides light. Thus, it is necessary to determine the refractive index depth distribution as accurate as possible.

So, in this paper, the Mach-Zehnder interferometry method and a computational imaging processing are used for the experimental determination of the refractive index depth distribution in order to calculate the previous parameters.

Some techniques are well-known and widely spread in order to determine the mode indices for integrated-optical waveguides e.g. those fabricated by the diffusion method, which can be examined by WKB approximation theory [Conwell, 1973; Taylor, 1972; Marcuse, 1973]. Also theoretical calculations were made for the analytical determination of the mode field distribution of an integrated-optical waveguide fabricated by the diffusion method [Conwell, 1973; Taylor, 1972; Marcuse, 1973]: for a waveguide with a refractive index profile varying exponentially with the depth, the mode field calculation yielded the Bessel function as the exact solution for TE modes.

In this paper, a series of optical waveguide samples is prepared at different process temperatures by the UV-laser lithographic method. For the purpose of increasing the measurement accuracy, the samples are examined

by the computer-based Mach-Zehnder interferometry method instead of the manually-based Mach-Zehnder contour line method in order to characterize the refractive index depth profile of the waveguide samples. Such an interferometric study based on image processing procedures is expected to yield more information about the refractive index modification zone inside the UV-irradiated polymeric material than in the former work, because the evaluation is not done manually by the contour lines method, but by the phase difference. The recorded interferograms are analyzed on the bases of FFT algorithm to extract the interference phase difference due to the refractive indices variations across the waveguides areas. The refractive index depth profile is studied at different process temperatures. The extracted interference phase difference variations along the irradiated area are presented in a 3D view. A mode field analysis is performed for the studied waveguides at different process temperatures. To use such kind of waveguides in integrated optics devices, it is useful to know the number of modes and their propagation coefficients for any given refractive index depth profile. As the propagating modes depend on the refractive index distribution in the optical waveguides zone, the mode numbers and their propagation coefficients are investigated for the given refractive index profile. Moreover, the attenuation of the propagated waves can be controlled based on this study. Finally, the best conditions to be applied in the fabrication process for such PMMA material are recommended.

Experimental Arrangement

Waveguide Sample Preparation

The waveguide samples are prepared using a UV laser contact mask irradiation lithographic method. Thus the integrated-optical waveguides are inscribed into the planar slabs of homogeneous PMMA [Shams-Eldin, 2005]. More experimental details are given in [Shams-Eldin, 2004; Shams-Eldin, 2005; Wochnowski, 2008; Wochnowski, 2005]. A Kr excimer laser is used at a wavelength of 248 nm. As a lithographic mask, a quartz glass on which a chrome layer with an inherent linearly-shaped strip aperture is sputtered is employed. The linearly formed strip aperture has a width of 150 μm . Before the UV-irradiation starts, the mask is directly positioned onto the surface of the planar PMMA slab substrate (contact mask method). A specially prepared holder is used to position the UV-lithographic on the sample. Figure (1) illustrates the shape of the cross sectional area of the fabricated

optical waveguide. After that, a temperature controller is employed to control the temperature of the sample during the irradiation process. A set of waveguides is prepared at different temperatures. The process parameters for waveguide fabrication for each sample (irradiation parameters like fluence, repetition rate and total number of pulses as well as the process temperature) are explicitly stated in section 3.1.

Measurement and Calculation of the Refractive Index Depth Profile

The refractive index depth profile of the prepared waveguide is described in figure (2). This figure presents the refractive index depth profile of a double layer waveguide [Karthé, 1991; Lin, 2009]. A double layer waveguide is featured by two distinct refractive index maxima located in different depths of the waveguide. The two distinct refractive index maxima are separated by a distance of a few μm . It looks like if two waveguides (a top one and a bottom one) are placed; one below the other in a parallel way. If light is coupled into the top waveguide, generated propagation modes propagate inside the top waveguide. But the coupling between the top and bottom waveguides is very strong due to the evanescent field and the short distance between both waveguides. Thus light energy is coupled from the top waveguide to the bottom waveguide generating radiation modes in the bottom waveguide, and the light energy is emitted continuously from the bottom waveguide into the surrounding leading to a high loss rate of such kind of waveguides.

Mach-Zehnder-interferometer is used to investigate the prepared waveguide samples, see figure (3). Mach-Zehnder-Interferometer comprises two arms; a reference arm and a probe arm. In the probe arm, the waveguide sample is dipped into a cuvette which is filled by an immersion liquid with refractive index n_l , which is matching with the refractive index n_s of the PMMA substrate. Thus the obtained interferogram only contains information about the UV-modified area of the waveguide sample (the pure waveguide). The collimated object beam crosses the sample and passes through the microscope objective MO1 with magnification 10X and a numerical aperture 0.25. An identical microscope objective MO2 is installed in the reference arm to eliminate the curvature of the optical field. The position of MO2 is precisely adjusted. The produced interferograms are recorded by an Allied Vision Marlin F145B2 CCD camera with pixel pitch 4.65 $\mu\text{m} \times 4.65 \mu\text{m}$ and pixel numbers 1392 in horizontal and 1040 in vertical direction.

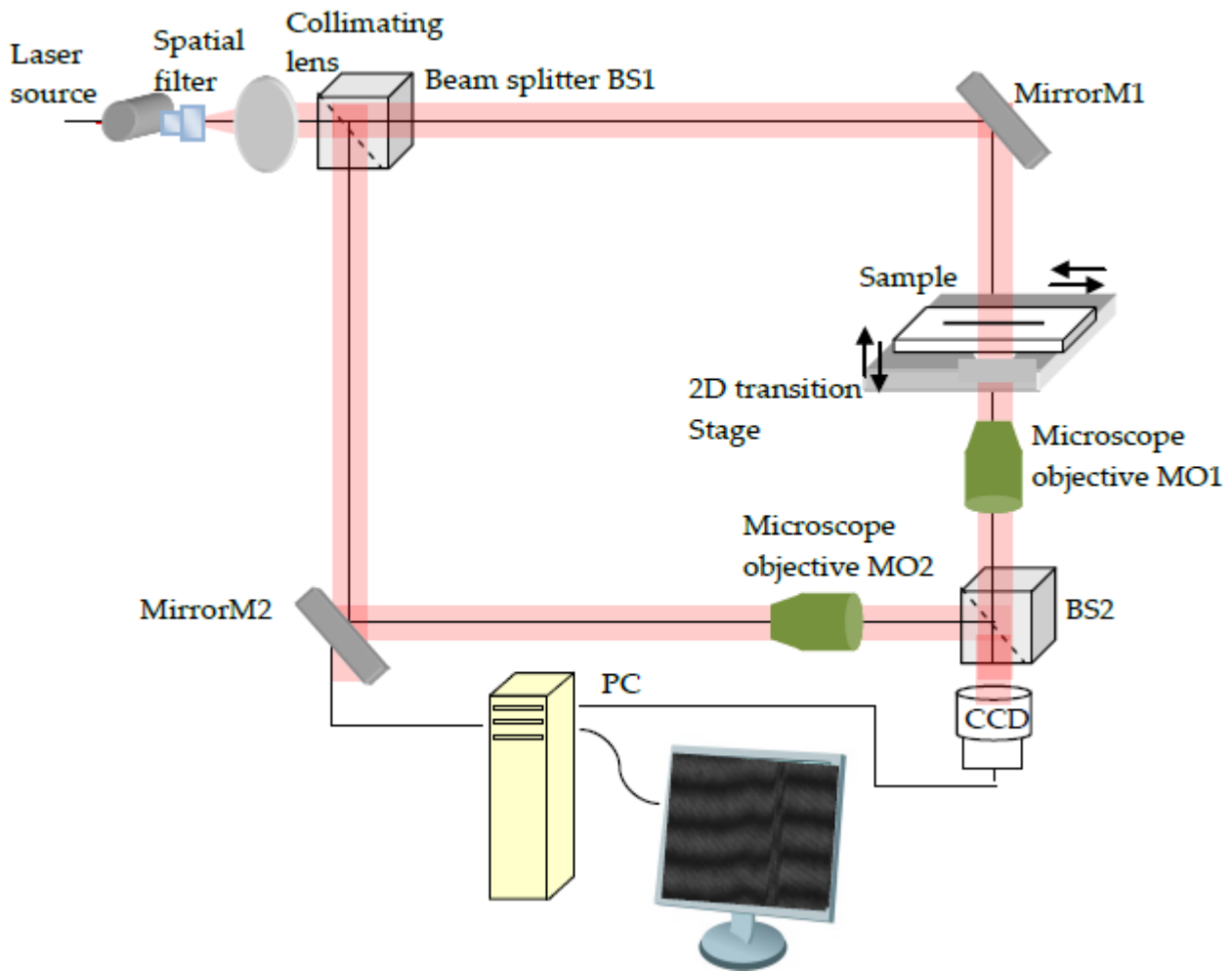


FIGURE 3 ARRANGEMENT OF THE USED TWO-BEAM INTERFEROMETER.

However, the UV irradiation lithographic method is used to inscribe optical waveguide in a slab of PMMA. The original homogeneous material surrounds the modified area of the used PMMA slab, where the refractive index of the used PMMA slab is n_s . The cross sectional area of the waveguide is divided into Q layers; figure (1). The refractive index of each layer is constant. The refractive index of the i^{th} layer is n_i , where $i=1,2,\dots,Q$. In addition, the thickness of each layer is constant. The refractive index variation extends into the polymer slab up to depth d . The layer thickness is equal to d/Q . The irradiated PMMA slab is immersed in matching liquid and then used in Mach-Zehnder interferometer. The object beam crosses the irradiated PMMA slab, the object beam and reference beam superpose. The produced interference pattern contains a field distribution which is related to the refractive index variations inside the modified area. The optical interference phase difference due to each layer depends on the refractive index n_i and is given by

$$\frac{\Delta\phi_i}{2\pi} \lambda = (n_i - n_s) a_i \quad , i = 1, 2, 3, \dots, Q \quad (1)$$

where a_i is the width of the i^{th} layer of the waveguide, and λ is the wavelength of the used light beam. The refractive index of PMMA slab (non-irradiated area) n_s is equal to the refractive index of the immersion liquid n_L .

The optical interference pattern is analyzed using FFT algorithm. The phase map of the interference field is calculated, and so the wrapped interference phase map is unwrapped. The unwrapped phases are normalized with respect to the background interference phase to extract the optical phase differences across the irradiated area, and then equation (1) can be used to calculate the refractive index n_i . Furthermore, the photo induced refractive index profile across the modified area is calculated using the full interference phase difference map.

Results and Discussion

Refractive Index Depth Profile

The prepared waveguide samples are now characterized by the above described Mach-Zehnder-interferometer techniques.

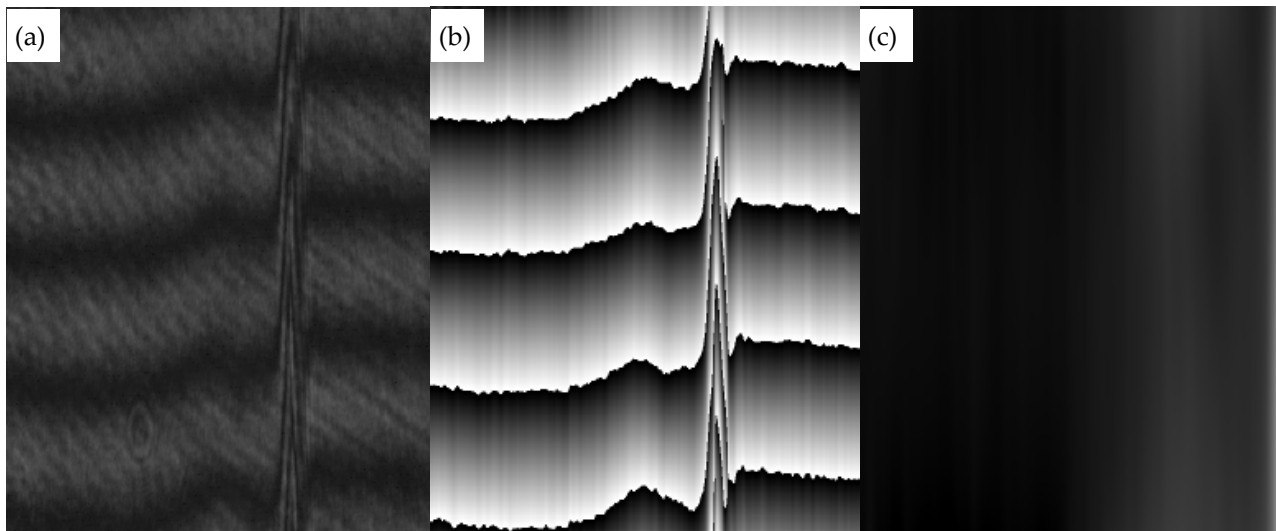


FIGURE 4 THE PRODUCED TWO-BEAM INTERFEROGRAM, (b) THE CALCULATED INTERFERENCE PHASE USING FFT ALGORITHM AND (c) THE EXTRACTED INTERFERENCE PHASE DIFFERENCE DUE TO THE FABRICATED WAVEGUIDE AT TEMPERATURE 22°C.

The first waveguide sample is prepared at a wavelength $\Lambda = 248 \text{ nm}$, by a fluence $f = 32 \text{ mJ/cm}^2$, a repetition rate $R = 5 \text{ Hz}$ and with a number of pulses $N = 1500$ pulse, and at a temperature T of 22°C (room temperature). This sample is immersed in a fluid of refractive index $n_L=1.4917$ perfectly matching the index of the substrate. The produced interferogram is shown in figure (4-a). The FFT algorithm is used to analyze this interferogram. The reconstructed interference phase distribution modulo 2π is displayed in figure (4-b). The phase map after unwrapping and subtraction of the monotonous background is calculated; figure (4-c). The extracted optical interference phase difference resulting from the refractive indices variations inside the optical waveguide is displayed in the three dimensional reconstruction; figure (5). The mean interference phase difference across the optical waveguide is combined with equation (1) to calculate the refractive index depth profile through the waveguide area; figure (6). Apparently, the refractive index depth profile is divided into two zones. At a temperature of 22°C , a two-layer waveguide is formed by UV-irradiation ($\Lambda = 248 \text{ nm}$) [Karthe, 1991]. The refractive index at the substrate surface is increased in comparison to the non-irradiated original polymeric material. However, with increasing depth, the refractive index drops until it reaches a local refractive index minimum ($n_{\text{mini}} \approx 1.4925$) at a depth ranging from $18.6 \mu\text{m}$ to $23.72 \mu\text{m}$. Then the refractive index increases again with rising depth until it reaches a local refractive index maximum at a depth of $55.33 \mu\text{m}$, which, however, is inferior to the surface refractive index. Then the refractive index starts again to fall until reaching the value of non-irradiated polymeric material at a depth of $113 \mu\text{m}$.

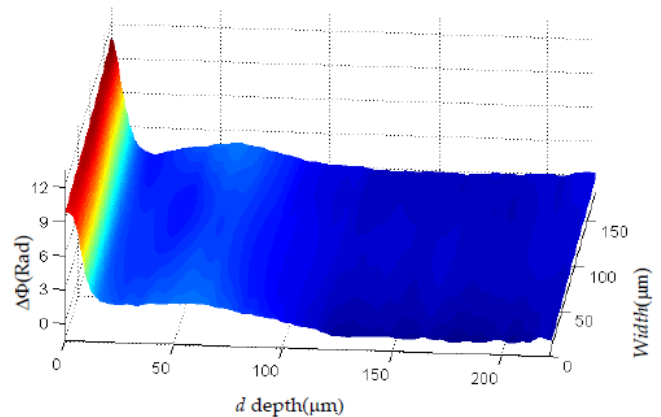


FIGURE 5 THE THREE DIMENSIONAL RECONSTRUCTION OF THE OPTICAL PHASE DIFFERENCE DISTRIBUTION FOR THE FIRST SAMPLE.

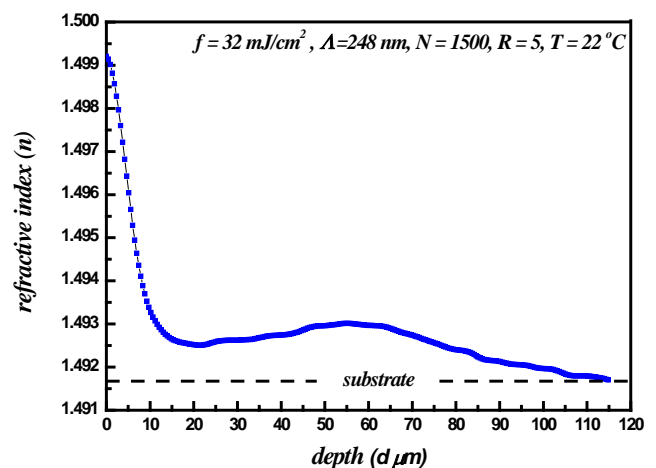


FIGURE 6 THE REFRACTIVE INDEX DEPTH PROFILE OF THE FABRICATED OPTICAL WAVEGUIDE AT $\Lambda = 248 \text{ nm}$, $F = 32 \text{ mj/cm}^2$, $R = 5 \text{ Hz}$, AND $T=22^\circ\text{C}$.

The same evaluation procedure is applied for the second waveguide sample prepared at a temperature 30°C with the same irradiation parameters. The produced interferogram is used to calculate the optical interference

phase difference across the modified area. Figure (7-a) shows the interferogram of this sample. The FFT is employed to calculate the interference phase distribution; figure (7-b). Figure (7-c) represents the extracted optical phase difference due to the fabricated waveguide. In addition, figure (8) represents the extracted interference optical phase difference distribution in three-dimensional reconstruction.

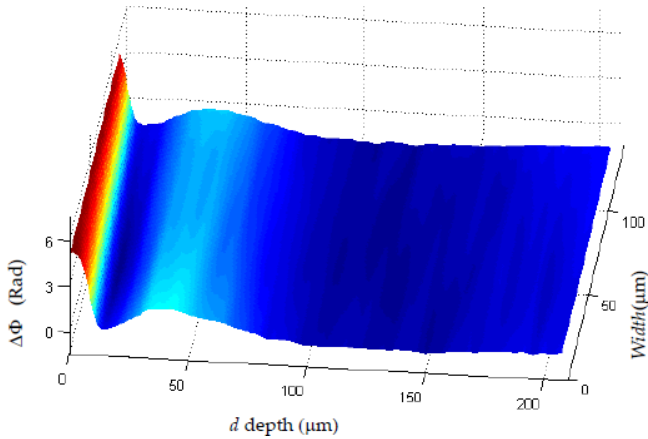


FIGURE 8 THE THREE DIMENSIONAL RECONSTRUCTION OF THE OPTICAL PHASE DIFFERENCE DISTRIBUTION FOR THE SECOND SAMPLE.

Further samples are prepared by the same irradiation parameters, but at different temperatures ($T = 40^{\circ}\text{C}$, 45°C , 50°C , 55°C and 60°C). All samples are evaluated by the same procedures. The refractive index depth profile calculation shows that the refractive index depth profile strongly depends on the temperature as shown in figure (9). Figures (9, a-e) represent the refractive indices depth profiles at temperatures 30°C ,

40°C , 45°C , 50°C , 55°C and 60°C . They are similar except for the local refractive index minimum as well as the highest refractive index on the top surface of the waveguide. TABLE 1 summarizes the difference between the calculated refractive indices maxima and minima of the top part at different temperatures. In figure (9-c), one can observe that the local refractive index minimum ($n_{\text{mini}} \approx 1.4918$) at temperature 45°C is more pronounced than that in the case at 22°C . This has a huge impact for the waveguiding effect of the waveguide structure. However, it is deepened on the local refractive index minimum and the refractive index at the top. Both waveguides (the top and the bottom one) of the two-layer-waveguide are supposed to be decoupled, so that no radiation modes occur in the bottom part when light is coupled into the top part of the waveguide and thus the loss rate of the waveguide is reduced [Wochnowski, 2008; Karthe, 1991; Lin, 2009]. At higher temperatures, the value of the refractive index of the local refractive index minimum and the refractive index at the surface changes with the processing temperature.

TABLE 1

T C°	$\Delta n \times 10^{-3}$
22	6.71
30	3.77
40	3.4
45	5.02
50	4.75
55	4.23
60	3.07

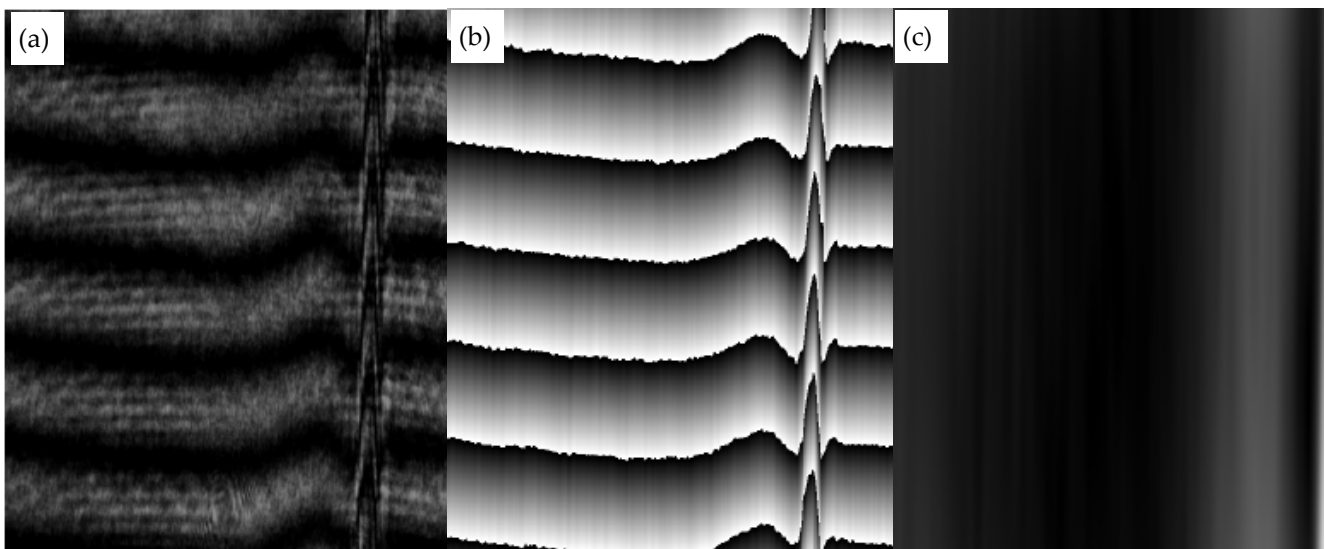


FIGURE 7 THE PRODUCED TWO-BEAM INTERFEROGRAM, (b) THE CALCULATED INTERFERENCE PHASE USING FFT ALGORITHM AND (c) THE EXTRACTED INTERFERENCE PHASE DIFFERENCE DUE TO THE FABRICATED WAVEGUIDE AT TEMPERATURE 30°C .

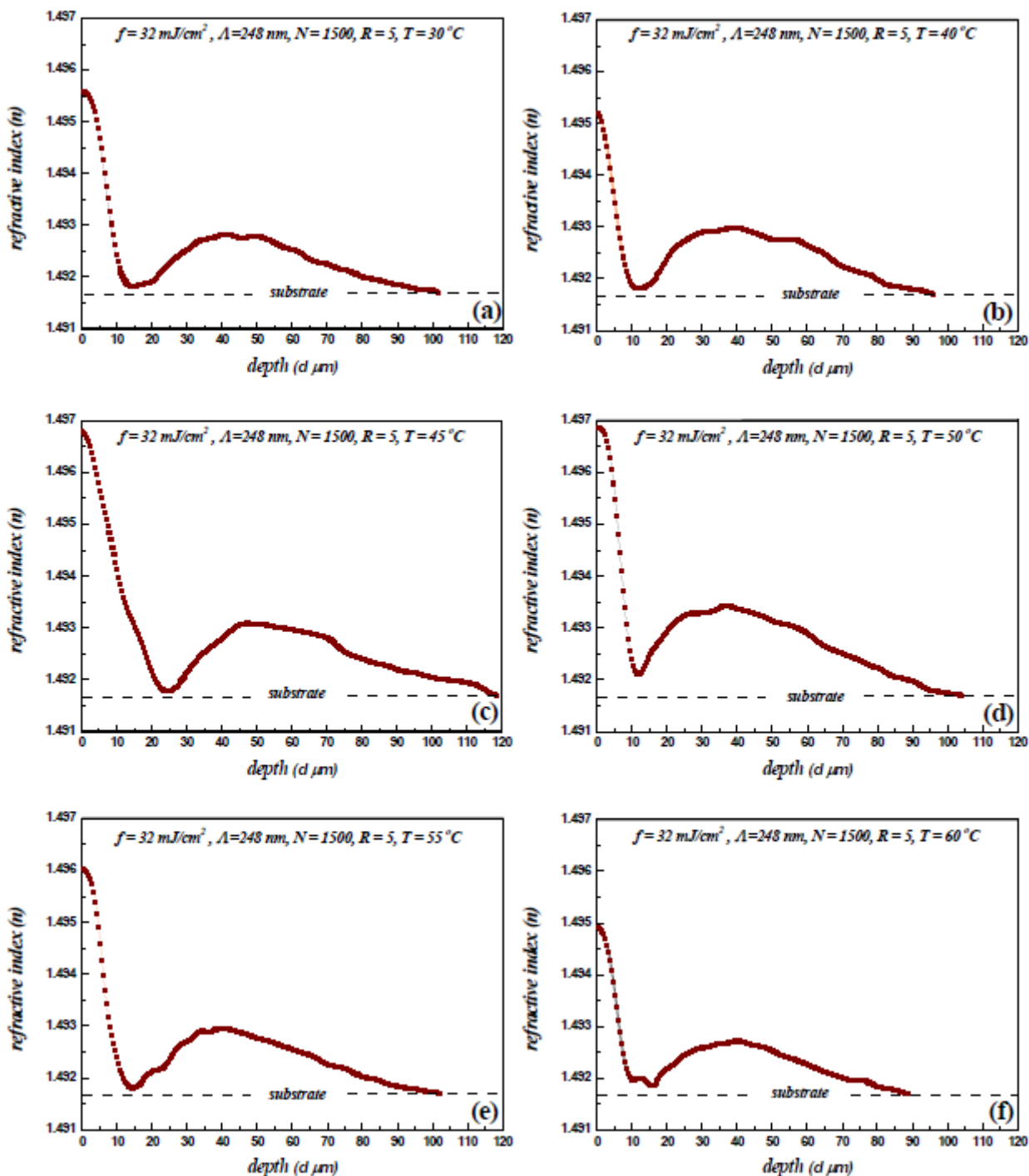


FIGURE 9 THE MEASURED REFRACTIVE INDICES PROFILES AGAINST THE DEPTH AT DIFFERENT TEMPERATURES FOR SAMPLES PRODUCED AS FOLLOWS: $\lambda = 248 \text{ nm}$, $f = 32 \text{ mJ/cm}^2$, $R = 5 \text{ Hz}$, and $T =$ (a) 30, (b) 40, (c) 45, (d) 50, (e) 55 AND (f) 60°C.

UV-photo-chemical Mechanism

A basic discussion about the UV-photon induced reaction mechanisms in PMMA material is given in [Wochnowski, 2000; Wochnowski, 2008; Wochnowski, 2005]. In [Wochnowski, 2000; Wochnowski, 2005] the UV-photon induced reaction mechanisms are discussed for room temperature ($T_R \approx 20^\circ\text{C}$), while in [Wochnowski, 2008] the UV-photon induced reaction mechanisms are discussed for a processing temperature near or slightly above the glass temperature ($T_G \approx 90^\circ\text{C}$) of the PMMA

polymer. But nowhere an investigation or discussion is published about the UV-photon induced reaction mechanisms in PMMA at a processing temperature which lies inside the temperature interval between the room temperature T_R of 20°C and the glass temperature T_G of 90°C as it is done in this work.

One can conclude from figure (9) that there is no regular (increasing or decreasing) behaviour of the refractive index change with temperature in the temperature interval from 30°C to 60°C . This is a clear

indication that not only one, but several different UV-photon induced processes occur at different moments at different temperatures and at different depths inside the PMMA bulk material during the UV-irradiation period. Some processes are supposed to decrease the refractive index, while other processes are supposed to increase the refractive index. All these UV-photon induced processes are competing with one another yielding the extraordinary refractive index depth profile and its temperature dependency as shown in figure (9).

TE Modes Determination

Our aim in this section is to find the allowed TE modes and the propagation coefficients of the waveguides β with a Gaussian refractive index profiles. It is assumed that the waveguide (figure (2)) consists of two graded index regions; both of which are supposed to have a Gaussian refractive index profile. The first region is $0 < z < d_1$, and the second one is $d_2 < z < d_4$. There is a very thin layer $d_1 < z < d_2$ of constant refractive index n_{s1} . The point $z = 0$ represents the interface between the surface of the first region of the waveguide, the immersion liquid of refractive index n_L , and the point $z = d_4$ represents the interface between the second region of the waveguide and the medium which is identical with the substrate, having the refractive index n_{s2} .

1) The First Region of the Refractive Index Depth Profile (upper part)

The refractive index profile through the first region of the waveguide in the range $0 < z < d_1$ is represented by the polynomial series,

$$n(z) = A_0 + A_1 z + A_2 z^2 + A_3 z^3 + A_4 z^4 + \dots \quad (2)$$

where $A_0, A_1, A_2, A_3,$ and A_4 are constants.

The condition for the wave propagation along the first region of the waveguide is a zigzag of the beam path and the total phase change must be a multiple of 2π . Using WKB approximation [Marcuse, 1973; Mathey, 1995], the lateral resonance condition for the first region is given by

$$2 \int_0^{d_1} \sqrt{k_o^2 n^2(z) - \beta_1^2} dz - 2\Phi_{1/2} - 2\Phi_{1/3} = 2m\pi, 1 \leq m \leq M \quad (3)$$

where $\beta_1 = k_o n_m$ is the propagation constant of the m^{th} mode; m is an integer. M is the total number of modes, $k_o = 2\pi/\lambda$ is the wave-vector, λ is the wavelength, n_m is the effective mode indices that propagates along the guide. $\Phi_{1/2}$ and $\Phi_{1/3}$ are the phase changes at the film-liquid interface and at the first and second regions interface, respectively.

Generally, these last quantities are approximated by $\Phi_{1/2} \approx \pi/2$ and $\Phi_{1/3} \approx \pi/4$ [Mathey, 1995].

The effective indices (n_m) of the first region are obtained numerically by introducing equation (2) into equation (3).

2) The Second Region of the Refractive Index Depth Profile (lower part)

Referring to figure (2), it is supposed that without loss of generality, the second region of the waveguide in the range $d_2 < z < d_4$ is divided into two asymmetric parts, which has an individually Gaussian refractive index profiles. The first and the second parts are within the ranges $d_2 < z < d_3$ and $d_3 < z < d_4$, respectively.

The refractive index profile through these two parts of the second region of the waveguide is represented by the following form

$$n(z) = \begin{cases} n_{s1} + \Delta n_2 e^{-\left(\frac{z-z_c}{d}\right)^2}, & d_2 < z < d_3 \\ n_{s2} + \Delta n_3 e^{-\left(\frac{z-z_c}{d}\right)^2}, & d_3 < z < d_4 \end{cases}, \quad (4)$$

where d is the irradiation depth for both, the first part between d_2 and d_3 , and the second part between d_3 and d_4 . Δn_2 is the difference between the refractive indices at the interface between the first and the second part at $z = d_3$ and that at $z = d_2$, whereas Δn_3 is the difference between the refractive indices at the interface between the first and the second part at ($z = d_3$) and that of the substrate at ($z = d_4$). At $z = d_3$, we get

$$n_{s1} + \Delta n_2 = n_{s2} + \Delta n_3 \quad (5)$$

Similarly and in analogy with equation (3), the lateral resonance condition for each part can be obtained.

For the first part, we have,

$$2 \int_{d_2}^{d_3} \sqrt{k_o^2 n^2(z) - \beta_{21}^2} dz - 2\Phi_{1/3} = 2m\pi, 1 \leq m \leq M \quad (6)$$

and the second part, we have,

$$2 \int_{d_3}^{d_4} \sqrt{k_o^2 n^2(z) - \beta_{22}^2} dz - 2\Phi_{1/3} = 2m\pi, 1 \leq m \leq M \quad (7)$$

where

$$\beta_{21} = k_o n_{21m} \text{ and } \beta_{22} = k_o n_{22m}. \quad (8)$$

β_{21} and β_{22} are the propagation coefficients of the m^{th} mode in the first and the second parts, respectively. n_{21m} and n_{22m} are the effective indices of the m^{th} mode in the first and second parts, respectively. The indices 21 and 22 refer to the first

and second parts of the second region.

The effective indices n_{1m} and n_{2m} of the first and second parts of the second region are obtained numerically by using equations (4), (6) and (7).

Now we calculate the effective indices associated with each TE mode. The guiding condition for the first region is represented by,

$$n_{s1} < \frac{\beta_1}{k_o} < n_{s1} + \Delta n_1 \tag{9}$$

Also the guiding conditions for the second region, for the first and second parts are represented respectively by,

$$n_{s1} < \frac{\beta_{21}}{k_o} < n_{s1} + \Delta n_2 \tag{10}$$

$$n_{s2} < \frac{\beta_{22}}{k_o} < n_{s2} + \Delta n_3 \tag{11}$$

Equations (4), (6) and (7) can be used to calculate the effective indices of each mode for every part of the second region. The first region of the first and the second samples support five modes, while that of the third sample supports three modes. Also, the first region of the fourth sample, which represents the top of the group, supports seven modes. All remaining samples support three modes for each one. The effective indices against the mode number are shown in figure (10). It has been shown that in case of TE modes, the effective indices decrease with increasing mode number in a non-linear way that the decline grows clearer and clearer with rising mode numbers.

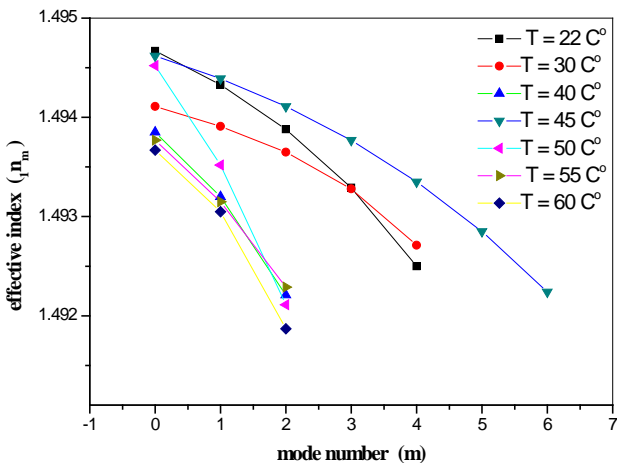


FIGURE 10 EFFECTIVE INDICES AGAINST THE MODE NUMBER OF THE FIRST REGION OF THE WAVEGUIDES FABRICATED BY A UV EXCIMER LASER AT A WAVELENGTH OF 248 nm, AND REPETITION RATE R IS 5 HZ, THE FLUENCE IS 32 mJ/cm² AND THE NUMBER OF PULSES IS 1500, AT DIFFERENT TEMPERATURES.

Generally, the number of the modes and the values of the effective indices depend on two factors, the

first of which is the depth, while the other is the refractive index difference Δn , both influenced by the process temperature. The first part of the second region supports four modes for all samples except for the fourth and seventh samples which support three modes as shown in figure (11). In addition, the second part of the second region supports modes in the range starting from six to eleven according to the depth of this part; which is shown in figure (12). As the case of the first region, also in the case of the second region, the effective indices decrease with increasing mode numbers in a non-linear way. But in case of the second region, the effective indices are lower than those in the case of the first region.

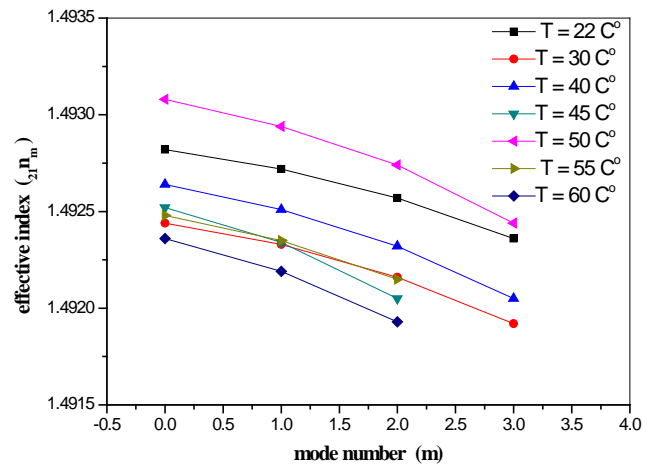


FIGURE 11 EFFECTIVE INDICES AGAINST THE MODE NUMBER OF THE FIRST PART OF THE SECOND REGION OF THE WAVEGUIDES FABRICATED BY A UV- EXCIMER LASER AT A WAVELENGTH OF 248 nm, AND REPETITION RATE R IS 5 Hz, THE FLUENCE IS 32 mJ/cm² AND THE NUMBER OF PULSES IS 1500, AT DIFFERENT TEMPERATURES.

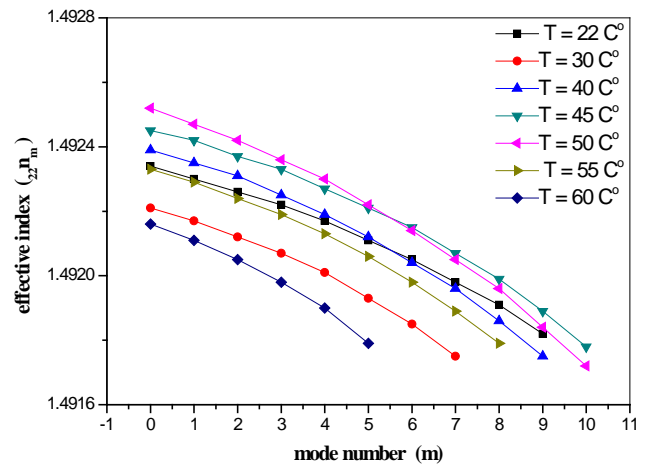


FIGURE 12 EFFECTIVE INDICES AGAINST THE MODE NUMBER OF THE SECOND PART OF THE SECOND REGION OF THE WAVEGUIDES FABRICATED BY A UV- EXCIMER LASER AT A WAVELENGTH OF 248 nm, AND REPETITION RATE R IS 5 Hz, THE FLUENCE IS 32 mJ/cm² AND THE NUMBER OF PULSES IS 1500, AT DIFFERENT TEMPERATURES.

Conclusion

It has been shown that the refractive index depth profile of the integrated-optical waveguides fabricated by the temperature-based UV-laser lithographic method strongly depends on the processing temperature. Thus the refractive index depth profile and thereby the mode field distribution, mode numbers and effective indices and other physical-optical and functional properties like the loss rate can be controlled by the process temperature. Mainly, the refractive index depth profile is strongly influenced by the process temperature: the existence of two refractive index maxima (a big one near the surface and a smaller one deep in the polymeric bulk material) and thereby the existence of a refractive index minimum between both maxima has been experimentally verified by the Mach-Zehnder interferometric method and computer-based image processing procedures with a higher accuracy than that with the manually-based Mach-Zehnder interferometry contour line method. The accuracy of the measured optical phase difference can be further increased when using the FFT method. For instance, the experiments yield that in case of TE modes the effective indices decreases with increasing mode numbers in a non-linear way.

Therefore, this temperature-based UV-laser lithographic method can be used to fabricate integrated-optical waveguides with precisely selected parameters. Hence, the performance of such waveguides can be improved and optimized for the operation in micro-optical devices for special applications.

ACKNOWLEDGMENT

The authors would like to acknowledge the DFG for supporting the work financially in the frame of the Project with the Contract No. VO 530-27-1.

REFERENCES

- A. K. Baker, P.E. Dyer, Refractive-index modification of polymethylmethacrylate (PMMA) thin films by KrF-laser irradiation, *Appl. Phys. A* 57 (1993) 543.
- C. Wochnowski, M. Shams El-Din, Temperature-controlled UV-laser induced fabrication of planar polymeric waveguides, *Opt. and Laser Tech.* 40 (2008) 365-372.
- C. Wochnowski, M.A. Shams El-din, S. Metev, UV-laser-assisted degradation of poly (methyl methacrylate), *Polym. Stabil. Degrad.* 89(2) (2005) 252.
- C. Wochnowski, S. Metev, G. Sepold, UV-Laser-Assisted Modification of the Optical Properties of Polymethylmethacrylate, *Appl. Surf. Sc.* 154-155 (2000) 706.
- C.I. Lin, T. K. Gaylord, Attenuation and mode profile determination of leaky/lossy modes in multilayer planar waveguides by a coupling simulation method, *Appl. Opt.* 48 (2009) 3603.
- D. Marcuse, TE modes of graded-index slab waveguides, *IEEE J. Quantum Electron.* QE-9 (1973) 1000.
- E. M. Conwell, Modes in optical waveguides formed by diffusion, *Appl. Phys. Lett.* 26 (1973) 328.
- F. Vollertsen, C. Wochnowski, UV-Laser Assisted Fabrication of Integrated-Optical Waveguides, *CIRP Annals - Manufacturing Technology* 53 (2004) 199-202.
- H. F. Taylor, W. E. Martin, D. B. Hall, V. N. Smiley, Fabrication of single crystal semiconductor optical waveguides by solid state diffusion, *Appl. Phys. Lett.* 21 (1972) 95.
- H. H. Wahba, T. Kreis, Characterization of graded index optical fibers by digital holographic interferometry, *Appl. Opt.*, 48 (2009) 1573.
- H. Ma, A.K.-Y. Jen, L.R. Dalton, Polymer-Based Optical Waveguides: Materials, Processing, and Devices, *Adv. Mater.* 14 19 (2002) 1339.
- I. P. Kaminow, J. A. Carruthers, Optical waveguiding layers in LiNbO₃ and LiTaO₃, *Appl. Phys. Lett.* 22 (1973) 326.
- J. Crank, *the Mathematics of Diffusion*, New York: Oxford (1956).
- L. Eldada, L.W. Shacklette, Advances in polymer integrated optics, *IEEE J. Sel. Top. Quantum Electron.* 6(1) (2000) 54 - 68.
- M. Koerdt, Fabrication and characterization of waveguide and grating structures induced by ultraviolet radiation in polymers with a shortened writing process, *Proc. SPIE*, Vol. 7213 (2009) 72130Y.
- M.A. Shams-Eldin, C. Wochnowski, M. Koerdt, S. Metev, A.A. Hamza, W. Jüptner, Characterization of the optical-functional properties of a waveguide written by an UV-laser into a planar polymer chip, *Opt. Mater.* 27(6) (2005) 1138.
- M.A. Shams-Eldin, C. Wochnowski, S. Metev, A.A. Hamza, W. Jüptner, Determination of the refractive index depth profile of an UV-laser generated waveguide in a planar polymer chip, *Appl. Surf. Sc.* 236 1-4 (2004) 31.

- P. Mathey, P. Jullien, Numerical analysis of a WKB inverse method in view of index profile reconstruction in diffused waveguides, *Opt. Comm.* 122 (1996) 127.
- R. V. Schmidt, I. P. Kaminow, Metal-diffused optical waveguides in LiNbO₃, *Appl. Phys. Lett.* 25 (1974) 458.
- T. G. Giallorenzi et al., Optical Waveguides Formed by Thermal Migration of Ions in Glass, *Appl. Opt.* 12 (1973) 1240.
- W. Karthe, R. Müller, *Integrierte Optik*, Akademische Verlags-gesell-schaft Geest & Portig, Leipzig (1991) (Chapter 3).